JOURNAL OF MECHANICAL ENGINEERING AND SCIENCES (JMES)
ISSN: 2289-4659 e-ISSN: 2231-8380
VOL.14, ISSUE 1, 6417 – 6429
DOI: https://doi.org/10.15282/jmes.14.1.2020.17.0502

ORIGINAL ARTICLE

Comparison of different additive manufacturing patterns on the performance of rapid vacuum casting for mating parts via the Taguchi method

N. N. Mohd Mustafa[1], A. Z. Abdul Kadir[1*], N. H. Akhmal Ngadiman[1], A. Ma'aram[1] and K. Zakaria[1]

[1] School of Mechanical Engineering, Faculty of Engineering, Universiti Teknologi Malaysia, Skudai, 81310 Johor Bahru, Johor, MALAYSIA
Phone: +6075534564; Fax: +605566159

ABSTRACT – Rapid vacuum casting has been proven to be a successful method in producing high-quality parts in small series. However, a challenge lies in the selection of proper Additive Manufacturing (AM) technologies for the development of a master pattern for the vacuum casting process. Each AM technologies differ from one another in terms of dimensional accuracy, surface finish, cost and lead times. The aim of this study is to investigate the performance of casting mating parts based on different additive manufacturing patterns for small batch. Three types of AM-based patterns: Fused Deposition Modeling (FDM), Stereolithography (SLA) and Multi-Jet Fusion (MJF) were compared. The Taguchi method, Signal to Noise ratio (S/N), Analysis of Variance (ANOVA) and T-test were conducted in determining the optimized parameters. From the findings, curing time is shown to be a significant parameter for dimensional accuracy and surface finish. Dimensional deviation varies in different directions of parts. For surface finish, there was only a slight change from the master pattern whereas the surface roughness of casting parts decreased within the range 0.23% to 2.85%. Tolerance grades for the selected dimensions of the parts were in the permissible range, based on ISO286-1:2010. When using distinct kinds of AM patterns to create replacement components, design tolerance is needed. It was suggested to select AM technology similar to that had been used for the original components. Battery cover was selected as a case study to represent the mating application parts.

ARTICLE HISTORY
Revised: 21st Oct 2019
Accepted: 4th Nov 2019

KEYWORDS
rapid casting;
additive manufacturing;
vacuum casting;
batch production.

INTRODUCTION

The integration of Additive Manufacturing (AM) with casting processes can also be referred to as Rapid Casting (RC). RC has been utilized to produce prototypes, sacrificial patterns and final products for small series production. One of the AM roles in the RC process is to produce patterns for vacuum casting, investment casting as well as sand casting. In the context of vacuum casting, RC can also be termed as Rapid Vacuum Casting (RVC) and has the ability to mimic the master patterns from AM technologies with good dimensional accuracy and surface finish. When used mainly for small series production, RVC shows a reduction of cost compared to other manufacturing processes, such as machining [1] and injection molding [2].

The vacuum casting process produces a series of parts using a silicon rubber mold that has been fabricated with the aid of AM patterns. In general, the dimensional accuracy of the final parts is influenced by the dimensional accuracy of the AM-based pattern. In addition, the production cost of AM patterns is included in the total production cost of this integrated process. Therefore, different types of AM-based patterns result in different performances in the context of dimensional accuracy, surface finish, cost and lead times [3]. All these performance characteristics need to be considered when selecting the proper AM technologies prior to the vacuum casting process.

Many AM technologies have evolved since 1987, beginning with the emergence of stereolithography (SLA) [4]. Additive manufacturing exhibits design flexibility in manufacturability [5]. SLA makes it possible to produce ideal prototypes, patterns and parts. Researchers have completed many studies relating to the integrated process of vacuum casting with AM. For instance, Fused Deposition Modeling (FDM) patterns have been used to produce final parts, such as gear [6], Bluetooth cover [7], hip joints [8] and thin wall-cover [9]. FDM is the most popular AM technique for constructing prototypes and parts that can be used directly as final products [7, 8, 10]. On the other hand, application of SLA patterns has been widely adopted in the investment casting process. SLA patterns were used to replicate a series of sacrificial patterns for the investment casting process, such as turbine blades [11, 12] and turbine impellers [13]. A Selective Laser Sintering (SLS) pattern was used to facilitate the casting process of complex geometry (bores, horizontal, vertical and inclined surfaces) [14]. In summary, AM-based patterns integrated with vacuum casting provide greater throughput in producing complex final parts for small series production. A study by Vosniakos et.al [15] investigated the process chain in producing a one-off replacement part for a two-stroke model engine of a car using investment casting. However, there is no study regarding the final replacement of mating parts in the scope of RVC. In addition, previous studies focused only on the specific AM-based pattern. To date, there is no comparative study on the performance of casting parts based on different AM-based patterns, such as FDM, SLA and Multi-Jet Fusion (MJF) on the mating parts.

*CORRESPONDING AUTHOR | A. Z. Abdul Kadir | ainizuhra@utm.my

Mating component requires further investigation as a larger variation of dimensional accuracy may affect the functionality of the parts. Basically, tolerance is assigned for mating parts to fit together. It is still challenging to maintain dimensional accuracy of mating parts developed using RVC process within permissible tolerance. Tolerance is assigned so that two mating parts can fit together. It is challenging to maintain dimensional accuracy of mating parts within permissible tolerance. For example, larger variation of dimension may affect the functionality of the parts.

This paper aims to compare the functional performance of casting parts based on different AM patterns for small batch production of a final replacement mating part using vacuum casting. In addition, the analysis was conducted in terms of dimensional accuracy and surface roughness. Three different AM-based patterns – FDM, SLA and MJF – were used in this study. The Taguchi method was adopted in order to obtain optimal process parameters for the vacuum casting process. Based on previous studies, the Taguchi method was successfully utilized in the optimization of the vacuum casting process [7, 8, 16, 17].

MATERIALS AND METHODS

Experimental Method

Based on the flow of methodology in Figure 1, the process started with the CAD model of required patterns. This was then converted into an STL file before being printed. The patterns were then fabricated, followed by fabrication of the mold. Next, the casting resin was poured into the silicone mold and the functional performance of the rapid vacuum casting parts was measured in terms of dimensional accuracy and surface roughness. The response optimizer module in Minitab 17 was used to predict the optimal parameter of each response and a confirmation test was conducted. Subsequently, the same experimental method of the vacuum casting process was repeated on the SLA and MJF patterns using the optimized parameter. Analysis and evaluation of the three different AM-based patterns – FDM, SLA and MJF – were compared in terms of dimensional accuracy. Each stage of this rapid vacuum casting process is elaborated in the following sub-sections.

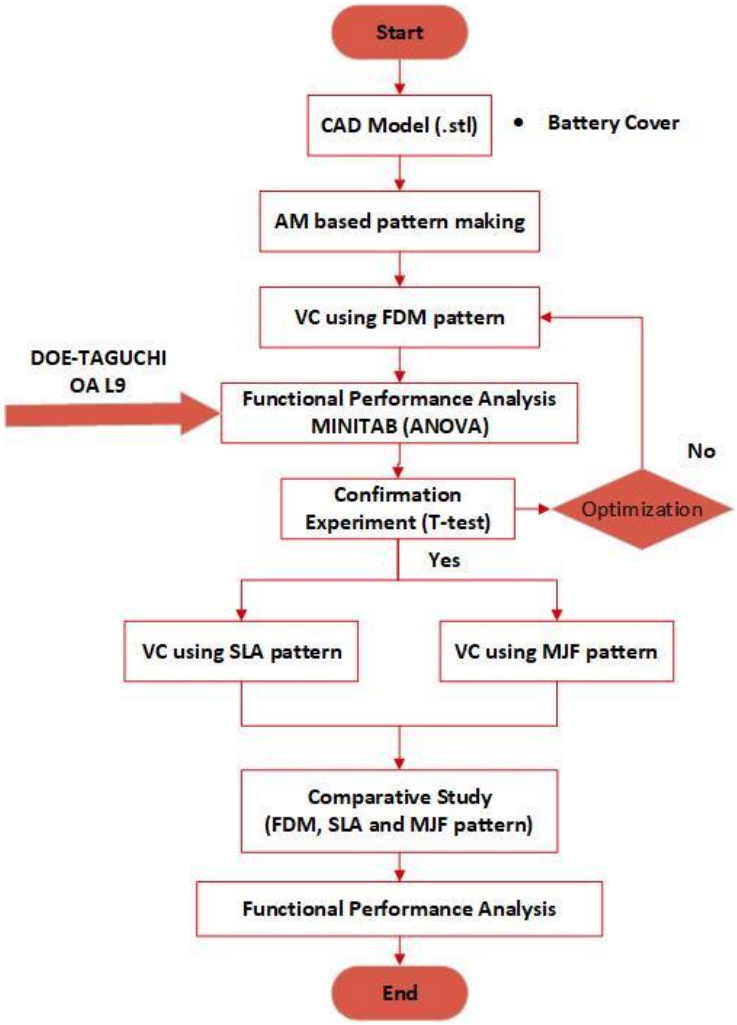

Figure 1. Methodology of process flow.

CAD Model

The geometry of the pattern used in this study is the battery cover of an enclosure. Figure 2 shows the CAD model designed in Solidworks, while Figure 3 shows the part measurement with two major sections denoted by A (26.84mm) and B (49.84mm). The thickness of the part is 1.5mm.

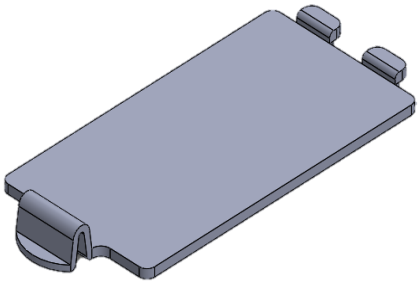

Figure 2. CAD model.

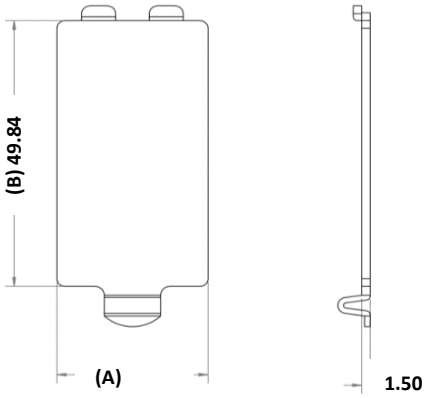

Figure 3. Part measurement drawing (mm).

Pattern Fabrication

Three types of pattern from different AM families as shown in Figure 4 were fabricated by FDM, SLA and MJF processes, respectively. Materials used for the fabrication of pattern are listed in Table 1.

Table 1. Types of pattern, materials and AM family.

Types of Pattern	Materials	AM Family
FDM	ABS	Material extrusion
SLA	Detailed resin white	Vat photopolymerization
MJF	Polyamide	Powder bed fusion

Figure 4. Three different AM patterns.

Mold Fabrication

Addition cured silicon rubber-J840 with mixing ratio 1:1 was used as mold material in this experiment. The addition of cured silicon rubber exhibited virtually no shrinkage compared to condensation cured rubber. Modeling clay technique was used to fabricate the silicone mold. The compatibility of the cured silicon rubber with polyurethane resin must be properly considered according to technical specifications from the manufacturer. The dimension of the mold was approximately 10.3 cm x 7.5 cm x 5 cm.

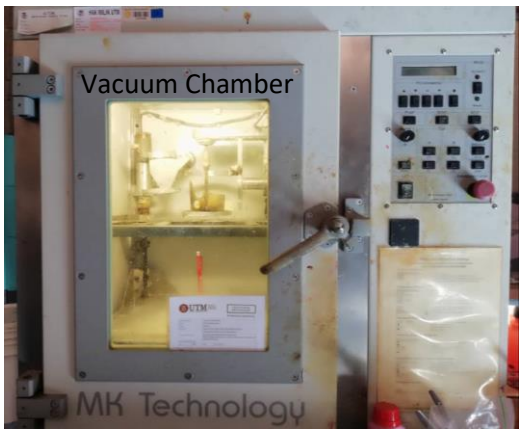

Figure 5. Vacuum casting machine.

Casting Resin

The resin used in this experiment is Alchemix VC 3392, which simulates the ABS properties. The amount of resin required was determined to be approximately 1.3 of the weight of the master pattern [18]. Before casting, the mold was preheated in an oven at 65◦C. In this study, ovens from MK Technology were used.The purpose of preheating the mold is to compensate for mold shrinkage [19]. Next, the part was cast in the vacuum chamber as shown in Figure 6 (a). The mold was moved from the vacuum casting machine into the oven for curing. After the resin had been cured, the casting part was removed from the silicone mold as well as the sprue and vents. The curing time depended on the size of the parts. The larger the part, the longer the curing time. The final casting part was obtained through this process and could be used as a functional part. The total time for VC processing, approximately 2.22 hours, was calculated based on the summation of preheating time, vacuum time and curing time.

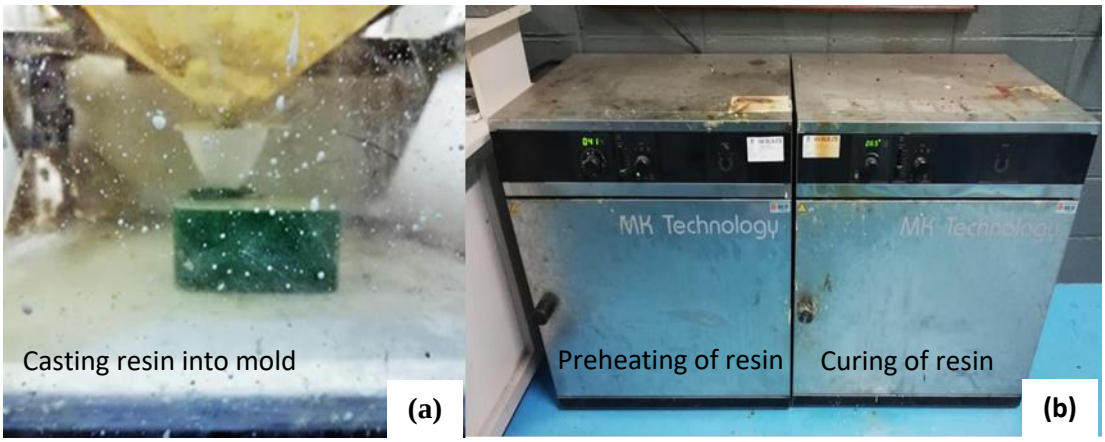

Figure 6. (a) Pouring the mixture of resin into silicone mold (b) Oven from MK Technology.

Processing Parameter

The Taguchi experiment method with three factors and three levels was implemented in this study to investigate the effect of casting parameters on the quality of the vacuum casting process in terms of dimensional accuracy and surface finish. Factors considered are preheating time, vacuum time and curing time, as shown in Table 2. These parameters were selected after several trials and errors during preliminary testing were performed. The range of these selected parameters are also in line with other studies [7, 8, 16]. Selection of suitable orthogonal array (OA) depends on the total number of degrees of freedom (DOF) of the processing parameters and levels. Therefore, L9 array was selected as the layout for this experiment.

Table 2. Selected processing parameters and level.

Serial	Factors	Levels		
		1	2	3
A	Preheating time (min)	30 (A1)	40 (A2)	45 (A3)
B	Vacuum time (min)	15 (B1)	18 (B2)	21 (B3)
C	Curing time (min)	45 (C1)	55 (C2)	65 (C3)

The parameter measurement was then performed in terms of dimensional accuracy and surface roughness.

Dimensional Accuracy

The dimensional accuracy of the casting parts was measured using the Mitutoyo PJ300 profile projector optical comparator. The dimensional deviation, *(Δd),* was calculated by comparing the dimension of the casting parts with the master pattern, as follows:

$$\Delta d = D_C - D_M \quad (1)$$

where D_C is the dimension of the casting part and D_m is the dimension of the master pattern.

Surface Roughness

The surface roughness value in terms of Ra (μm) was measured using a Mitutoyo surface roughness tester. Table 3 shows the parameter setting of surface roughness, showing stylus speed, cut-off length and sample size, with values 0.5mm/s, 0.25mm and 5, respectively.

Table 3. Parameter setting of surface roughness tester

Stylus Speed	Cut-off length	Sample Size
0.5 mm/s	0.25mm	5

RESULTS AND DISCUSSION

Dimensional Deviation and Surface Roughness

Figure 7 shows nine specimens of battery cover produced using the rapid vacuum casting process. They were labeled from samples one to nine to represent the different parameter settings. Table 4 shows the data collected for these nine specimens. From the results, Samples 2 and 3 showed a negative deviation on Dimension A, while the other samples showed a positive deviation. Meanwhile, all nine samples on Dimension B showed a negative deviation. The positive deviation refers to expansion, while the negative deviation refers to shrinkage. The maximum deviation value on Dimensions A and B were 0.106mm and 0.246mm, respectively. The results showed inconsistent values of dimensional deviation on the two sections, supporting the possibility that this may be due to the direction of filling in the silicone mold [11].

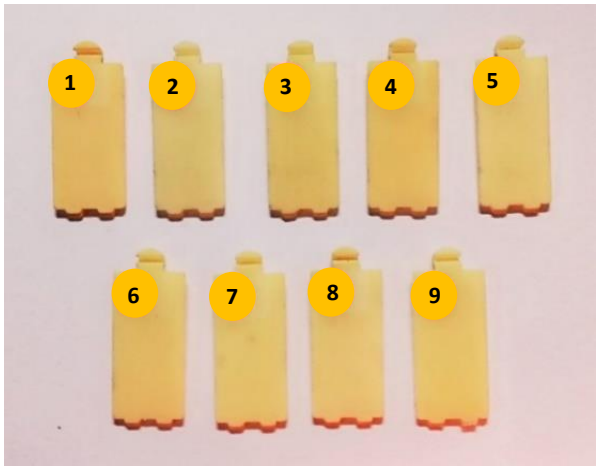

Figure 7. Nine samples of vacuum casting specimens.

In addition, for surface roughness, the Ra values for all samples were within the range of 21.445 µm to 22.025µm, while the measured surface roughness of the FDM pattern was 22.075µm. The surface roughness of casting parts decreased from master pattern about 0.23% to 2.85%. In contrast with the previous study, the Ra values for casting parts in this study were slightly reduced from the master pattern [8]. From the findings, the surface roughness of casting parts may increase or decrease slightly from the master pattern, depending on the type and properties of the material. The values of the surface roughness of casting parts produced using the master pattern that had undergone chemical vapour smoothing (CVS) processing were 0.319µm -0.667µm [8] and 0.455µm to 0.593µm [7] with ABS as casting material. It can be concluded that the casting parts produced from the master pattern with CVS processing showed a lower value of surface roughness compared to this study.

Table 4. Experimental results of L9 orthogonal array.

Sample No	Preheating Time (min)	Vacuum Time (min)	Curing Time (min)	Average deviation (mm)		Surface roughness, Ra (µm)
				A	B	
1	30	15	45	0.106	0.061	21.648
2	30	18	55	0.008	0.126	21.566
3	30	21	65	0.069	0.246	21.445
4	40	15	55	0.077	0.042	21.715
5	40	18	65	0.024	0.043	21.554
6	40	21	45	0.12	0.022	21.814
7	50	15	65	0.043	0.04	21.597
8	50	18	45	0.105	0.017	22.025
9	50	21	55	0.075	0.027	21.932

S/N Ratio Analysis

Minitab 17 software was used in data analysis and the values of Signal to Noise Ratio (S/N Ratio) were obtained. Since, the aim of this study to reduce deviation value and surface roughness, S/N ratio using a 'smaller is better' equation has been used. The term 'signal' represents the desirable value for the response characteristic and the term 'noise' represents the undesirable value for the response characteristic [20]. The graphs of the main effects of the signal to noise ratios were plotted. The S/N Ratio was calculated as in Equation. (2) as follows:

$$S/N = -10log_{10}\left[\frac{1}{n}\sum_{i=1}^{n} y_i^2\right] \quad (2)$$

where n is the number of repetitions and Y is the observed value of the response characteristic.

Figure 8 shows the main effects plot for S/N ratios for the average deviation (A). The plot indicates deviation (A) increases as preheating time increases due to the expansion rate of the mold. When the vacuum time is 18 min, deviation A is at minimum. Next, deviation A showed the optimum value when the time was at 55 min. The optimum parameter condition that minimized the deviation values were A1, B2 and C2.

Subsequently, Figure 9 shows the main effects plot for S/N ratios for the average deviation (B). The pattern of preheating time plot of deviation (B) is vice versa with the deviation (A). It can be seen that deviation (B) decreases with increased preheating time. For vacuum time, similar to deviation (A), the optimum parameter is when vacuum time is at 18min. The study of Ahmad *et.al* [16] showed the vacuum time was optimized at the minimum vacuum time. Deviation (B) decreases as curing time increases. The optimum parameter conditions that minimize the deviation values are A3, B2 and C1.

Figure 10 shows the main effect plot of S/N ratios for surface roughness. The surface roughness increases as preheating time increases. For surface roughness, the optimum parameter of vacuum time is at 15 min. Surface roughness is optimum when curing time is 65 min. In line with the previous study [7], the surface roughness decreases as temperature increases. The optimum parameter conditions that minimize the surface roughness are A1, B1 and C3. Descriptions for A, B and C are presented as in Table 2.

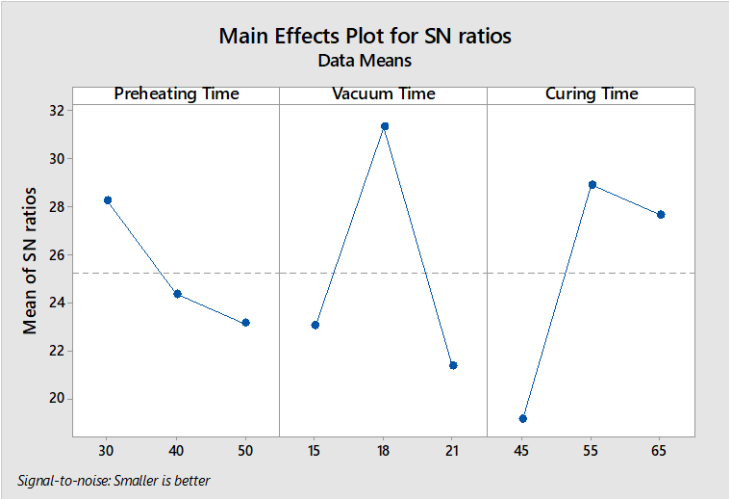

Figure 8. Main effect plot of S/N ratios for deviation (A).

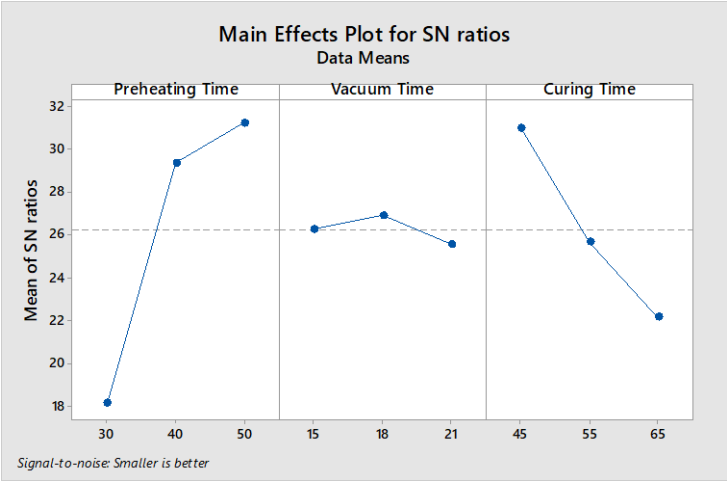

Figure 9. Main effect plot of S/N ratios for deviation (B).

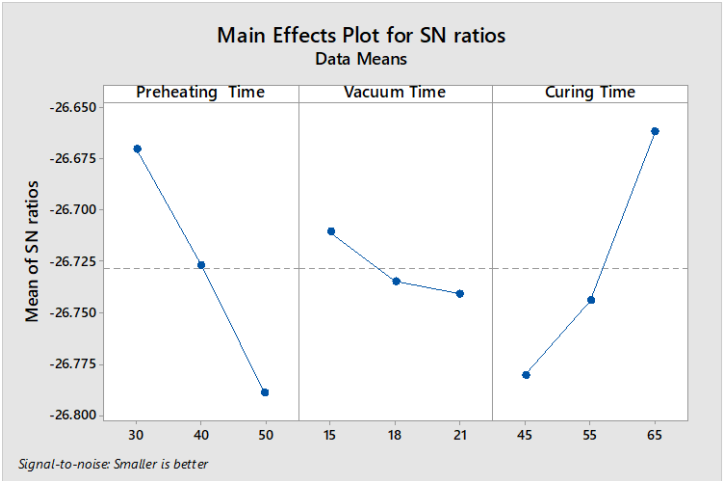

Figure 10. Main effect plot of S/N ratios for surface roughness.

ANOVA Analysis

Analysis of variance (ANOVA) was conducted to analyze the result of each response in the orthogonal experiment. Degree of freedom (DOF), significance and contribution of each parameter, sum of the squares of the deviation (SS), F-value and P-value were evaluated. P-values less than 0.05 showed that the model is statistically significant on deviation and surface roughness. Larger F-values of any factors showed that the variation in this factor causes a large variation in

performance characteristics. For deviations A and B, the curing time is significant, as the P-value is 0.006 and 0.009, which is less than 0.05, as shown in Tables 5 and 6, respectively. The contribution of curing time (48.40%) on surface roughness is more significant than the preheating time and curing time, as shown in Table 7. It can be seen that the effect of the error on deviation A, deviation B and surface roughness is very low compared to other control factors.

Table 5. ANOVA data for deviation (A).

Source	DOF	Contribution (%)	Adj SS	F-Value	P-Value
Preheating Time	2	2.82	0.001061	5.11	0.164
Vacuum Time	2	9.45	0.003553	17.10	0.055
Curing Time	2	87.17	0.032777	157.74	0.006
Error	2	0.55	0.000208		
Total	8	100.00			

Table 6. ANOVA data for deviation (B).

Source	DOF	Contribution (%)	Adj SS	F-Value	P-Value
Preheating Time	2	65.77	17.0219	216.83	0.005
Vacuum Time	2	1.91	0.4932	6.28	0.137
Curing Time	2	32.02	8.2861	105.55	0.009
Error	2	0.30	0.0785		
Total	8	100			

Table 7. ANOVA data for surface roughness.

Source	DOF	Contribution (%)	Adj SS	F-Value	P-Value
Preheating Time	2	46	0.131426	18.56	0.051
Vacuum Time	2	3.13	0.008932	1.26	0.442
Curing Time	2	48.40	0.138280	19.52	0.049
Error	2	2.48	0.007082		
Total	8	100			

Optimization and Confirmation Experiment

Response Optimizer in Minitab was used to identify the combination of input variable settings that optimize the individual responses [7]. The desirability specification with predetermined goals for vacuum casting is shown in Table 8. The predicted optimal solution was calculated with the desirability values, as shown in Table 9. The desirability value of 1 indicates the ideal case, and 0 indicates the responses outside the acceptable limits.

Table 8. Desirability specifications for vacuum casting

Name	Goal	Lower limit	Upper Limit
Preheating Time	Constrain to region	30	50
Vacuum Time	Constrain to region	15	21
Curing Time	Constrain to region	45	65
S/N Ratio (Deviation A)	Maximize	18.42	41.94
S/N Ratio (Deviation B)	Maximize	12.18	35.39
S/N Ratio (Surface roughness)	Maximize	-26.86	-26.63

Table 9. Predicted optimal conditions.

Factors			S/N Ratio Deviation (A)	S/N Ratio Deviation (B)	S/N Ratio Surface roughness	Composite Desirability
A	B	C				
50	18	65	38.75	30.08	-26.70	0.7624

Table 10 shows the confirmation experiment conducted using the predicted optimal conditions. It can be seen that the values of deviation (A), deviation (B) and surface roughness were consistent. As mentioned in the previous section, the maximum deviations of the casting part before optimization for Dimension A and B were 0.106 mm and 0.246 mm respectively. After optimization, the deviation decreases by about 64.15% and 80.08% for Dimension A and Dimension B, respectively. On the other hand, only a small percentage (1.62%) of reduction occurred on the surface roughness values. Singh et.al [7] calculated the predicted mean from the predicted S/N ratio values. The predicted mean was then compared and verified with the confirmation experiment results.

In this study, the predicted mean values were also calculated but were used in a T-test. The T-test was conducted to verify the confirmation experiment, as shown in Table 11. The mean for deviation A was 0.038 with 95% Confidence Interval (CI), 0.035 to 0.042. The p-value is 0.001, which is less than 0.05 and is statistically significant. The mean for deviation B was 0.049 with 95% CI, 0.036 to 0.062. The P value is 0.029, which is less than 0.05 and is also statistically significant. For surface roughness, the mean was 21.668 with 95% CI, 21.556 to 21.78. The P-value was not statistically significant for surface roughness as it is larger than 0.05. Similar to the study [7], there was only a slight change in surface roughness values after optimization. For example, before optimization the Ra values were in the range of 0.455µm to 0.593µm, and after optimization the values were 0.453µm and 0.485µm.

Table 10. Confirmation experiment.

Samples	Deviation A (mm)	Deviation B (mm)	Surface Roughness (Ra)
1	0.037	0.045	21.655
2	0.04	0.055	21.631
3	0.038	0.047	21.718

Table 11. T-test by Minitab 17.

Variable	N	Mean	Standard Deviation	SE Mean	95% CI	T	P
Deviation A	3	0.038	0.001528	0.000882	(0.035, 0.042)	30.43	0.001
Deviation B	3	0.049	0.00529	0.00306	(0.036, 0.062)	5.79	0.029
Surface Roughness	3	21.668	0.0449	0.0259	(21.556, 21.78)	1.16	0.367

IT Grades

As this study focuses on the mating part, the permissible tolerance for fits was considered. According to the International Organization for Standardization (ISO), the standard tolerances of IT grade for mechanical parts that require fit are within the range of IT5 to IT11 [21]. ISO tolerance grades were published as a guideline for designers. The measured dimension of casting parts was used to calculate the IT grade using Equation. (3) and Equation. (4) [22, 23]:

$$i = 0.45\sqrt[3]{D} + 0.001D \tag{3}$$

$$n_j = 1000\left(\frac{|D_{jN} - D_M|}{i}\right) \tag{4}$$

where i is the standard tolerance factors in μm, D is the geometric mean of the range of nominal size in mm, n_j is tolerance unit, D_{jN} is the nominal dimension which is referred to dimension of master pattern, and D_M is the measured dimension of casting parts.

The results showed that the calculated IT grades, based on ISO 286-1:2010 of the casting parts, were within the acceptable range of IT grades for fit, as shown in Figure 8. The standard basic size in this experiment is 18mm to 30mm for Section A, and 30mm to 50mm for Section B. For deviation A, samples 1, 3, 4, 8 and 9 showed IT 10 grade, while samples 5 and 6 recorded IT 7. Samples 2 and 7 showed IT 5 and IT 6, respectively. Overall, the inconsistent values of IT grades are on section A. For deviation B, samples 4, 5 and 7 recorded IT 8, while samples 2 and 9 were IT 10. For

samples 1, 3, 6 and 9 the IT grades were IT 9, IT 11, IT 6 and IT 5, respectively. Similar to section A, samples in section B also showed inconsistent values of IT grades prior to the optimization process.

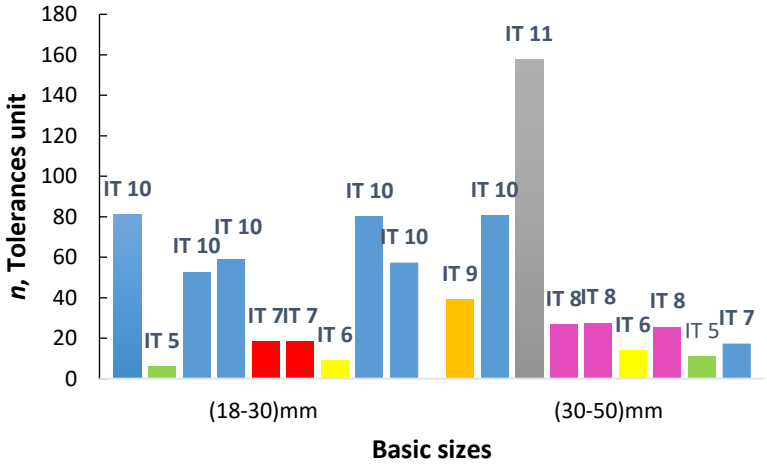

Figure 11. Dimensional accuracy of nine specimens in terms of IT grades.

Comparison of AM-Based Pattern

Dimensional Accuracy

The deviation values of the part produced by the FDM pattern using optimized parameter settings, as shown in the previous section, will also be discussed in this section. The dimension of the FDM pattern for dimension A is 26.704mm, and Dimension B is 49.352mm. Next, the dimension of the SLA pattern for Dimension A is 26.897mm and Dimension B is 49.977mm. Finally, for the MJF pattern, Dimension A is 27.065mm and Dimension B is 50.148mm. The deviation value is calculated as Equation. (5):

$$\Delta d = D_M - D_{CAD} \tag{5}$$

where D_m is the dimension of the master pattern and D_{CAD} is the dimension of computer aided design (CAD).

Figure 12 shows the deviation value of patterns from the CAD model. From the observation, the SLA patterns showed the lowest deviation value compared to FDM and MJF. In contrast, for section B, the FDM pattern showed the highest deviation value, followed by the MJF pattern and the SLA pattern.

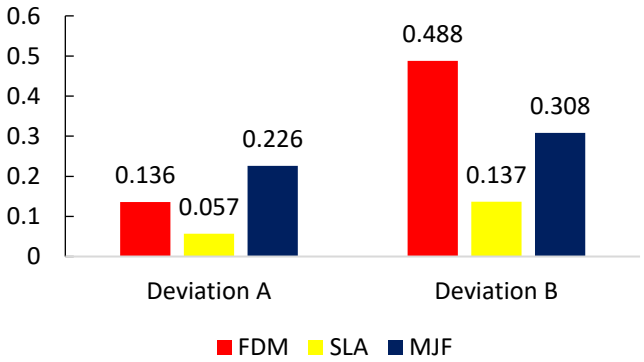

Figure 12. Deviation of AM-based patterns from the CAD model.

Experimental data for the casting parts, based on the three types of AM-based patterns – FDM, SLA and MJF – are shown in Tables 12, 13 and 14, respectively. It can be seen that for the FDM pattern, Dimension A of the casting parts has undergone expansion, as all three selected samples showed an increase in dimension. Meanwhile, Dimension B in the casting parts has undergone shrinkage within the range of 0.045mm to 0.055mm. Subsequently, both Dimensions A and B of the casting parts via the SLA pattern have undergone an expansion. The casting parts from the MJF pattern show the shrinkage values on sections A and section B. Figure 10 shows the final mating condition of the casting part, which shows that the battery cover fits well within the cavity of the enclosure. The dimensions labeled in Figure 10 represent the dimensions of the cavity of the enclosure.

Table 12. Experimental data for casting parts via the FDM pattern.

Samples	Dimension A (mm)	Deviation A (mm)	Dimension B (mm)	Deviation B (mm)
1	26.741	+0.037	49.307	-0.045
2	26.744	+0.04	49.297	-0.055
3	26.742	+0.038	49.305	-0.047

Table 13. Experimental data for casting parts via the SLA pattern.

Samples	Dimension A (mm)	Deviation A (mm)	Dimension B (mm)	Deviation B (mm)
1	26.924	+0.027	50.015	+0.038
2	26.922	+0.025	50.010	+0.033
3	26.921	+0.024	50.013	+0.036

Table 14. Experimental data for casting parts via the MJF pattern.

Samples	Dimension A (mm)	Deviation B (mm)	Dimension B (mm)	Deviation B (mm)
1	26.950	-0.115	49.951	-0.197
2	26.952	-0.113	49.955	-0.193
3	26.942	-0.123	49.946	-0.202

In relation to replacement parts, it was suggested that choosing the AM technology previously used to make the original parts was advisable, as different technologies would result in a different level of accuracy. From the observation, the battery cover produced from SLA and MJF patterns did not interlock well with the cavity of the enclosure due to the deviation on Dimension B. It can be seen that Dimension B of the SLA pattern deviates in a positive direction from the Dimension B cavity of the enclosure. The casting parts produced from the SLA pattern also deviate in a positive direction from the SLA pattern, increasing the deviation of Dimension B from the cavity. As a result, the positive deviation on Dimension B provided no clearance on these two mating parts. In addition, Dimension B of the MJF pattern also deviated in a positive direction from the Dimension B cavity of the enclosure. In comparison with SLA, the casting parts from the MJF pattern recorded a negative deviation. However, Dimension B still deviated in a positive direction from the Dimension B cavity of the enclosure. Similarly, with casting parts from the SLA pattern, the positive deviation on Dimension B also provided no clearance on the two mating parts from the MJF pattern. The significant of dimensional accuracy parts is very important as it help to produce better quality part as well as reduce material waste [24].

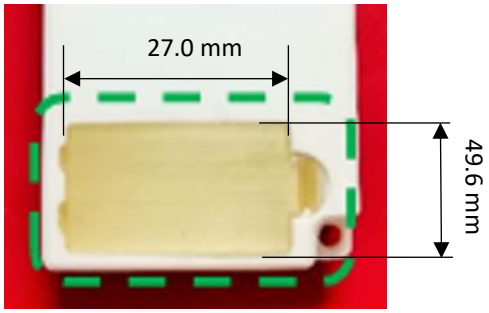

Figure 13. Battery cover interlocks on the cavity of the enclosure.

Surface Roughness

The surface finish for FDM, SLA and MJF pattern were 22.075 μm, 4.075 μm and 14.548 μm, respectively. Table 15 shows the surface roughness of casting parts. Results showed surface roughness (Ra) values for all the casting parts were lower than the measured surface roughness of the AM-based patterns, indicating that the properties of materials used caused a slight decrease of surface roughness values from the master pattern. For FDM, SLA and MJF, the surface roughness decreases from master pattern about 1.84%, 9.62% and 6.09%, respectively.

Table 15. Surface roughness of casting parts.

Surface Roughness (Ra) / Samples	Casting part – FDM	Casting part – SLA	Casting part – MJF
1	21.655	3.788	13.547
2	21.631	3.576	13.940
3	21.718	3.686	13.501

IT Grade

Table 16 shows the comparison of IT grade of casting parts from different patterns. For Dimensions A and B of the casting parts using the FDM pattern, the calculated tolerance grade was IT 8. The calculated IT grade for casting parts using the SLA pattern was IT 7. Finally, the calculated IT grade for casting parts using the MJF pattern was IT 11. IT differences of casting parts from different patterns may possibly due to variation size of AM patterns.

Table 16. IT grade for casting parts.

IT	Casting part – FDM		Casting part – SLA		Casting part – MJF	
Samples	Dimension A	Dimension B	Dimension A	Dimension B	Dimension A	Dimension B
1	IT 8	IT 8	IT 7	IT 7	IT 11	IT 11
2	IT 8	IT 8	IT 7	IT 7	IT 11	IT 11
3	IT 8	IT 8	IT 7	IT 7	IT 11	IT 11

These findings will serve as a base for future studies related to the performance of casting parts based on the AM patterns.

CONCLUSION AND FUTURE WORK

This research presents an early study of RVC process for mating components. The investigation in terms of dimensional accuracy and surface finish provides basement for future researchers to further investigate the application of RVC process. From the study, some conclusions can be drawn: the Taguchi method has been successfully utilized in determining the optimal parameter settings of every response (deviation and surface roughness) in the vacuum casting process. The response optimizer module in Minitab 17 has predicted the optimal parameters in the VC process with composite desirability of 0.7624. The optimal parameter settings for the control factors, preheating time, vacuum time and curing time were 50 min, 18 min and 65 min, respectively.

Before optimization, the tolerance grades of measured dimensions of the casting parts using the FDM pattern were within the range of IT 5 to IT 11 according to ISO286-1:2010. After optimization, the tolerance grade of the casting parts was IT 8, indicating that a consistent IT grade had been obtained.

For the FDM-based pattern, the average dimensional accuracy of the casting parts produced from the master pattern was +0.038mm for Dimension A and -0.049mm for Dimension B. The surface roughness was within the range 21.632 μm to 21.718μm and the tolerance grade was IT 8.

Subsequently, for the SLA-based pattern, the average dimensional accuracy of the casting parts produced from the master pattern was +0.025mm for Dimension A and +0.036 for Dimension B. The surface roughness was within the range 3.576μm to 3.788μm. The tolerance grade for the casting parts was IT 7.

Finally, for the MJF-based pattern, the dimensional accuracy of the casting parts produced from the master pattern was -0.117mm for Dimension A and -0.197 for dimension B. The surface roughness was within the range 13.501μm to 13.940μm. The tolerance grade for the casting parts was IT 11. The dimensional accuracy of final parts produced is acceptable as permissible tolerances and suitable to use as final parts for small batch production.

For future work, study of the capabilities of two mating components with features such as snap fit and holes will be conducted. The functionality of the mating parts will be measured in terms of dimensional accuracy.

In conclusion, dimensional deviation varies in different direction of parts. For surface finish, there is only slight change from the master pattern, possibly due to the properties of the materials used. Tolerance grades for the selected dimension of the parts were in the permissible range, based on ISO286-1:2010. Design tolerance is required when different types of AM patterns are being used to produce replacement parts, and it was suggested that choosing an AM technology similar to that used for the original parts was advisable, as different technologies result in different levels of accuracy.

ACKNOWLEDGEMENTS

The authors wish to acknowledge the funding support from Universiti Teknologi Malaysia under the Tier 1 Research University Grant (GUP) Vot.16H12 and UTM Transdisciplinary Research (UTM-TDR) Grant Vot. 06G11.

REFERENCES

[1] Ramos AM, Relvas C, Simo˜es JA. Vacuum casting with room temperature vulcanising rubber and aluminium moulds for rapid manufacturing of quality parts: a comparative study. Rapid Prototyping Journal. 2003;9(2):111-5.

[2] Zhu Z, Pradel P, Bibb RJ, Moultrie J. Economic analysis of plastic additive manufacturing for production of end use products: a preliminary study. Rapid Design, Prototyping & Manufacturing 2017.

[3] Pal D, Ravi B. Rapid tooling route selection and evaluation for sand and investment casting. Virtual and Physical Prototyping. 2007;2(4):197-207.

[4] Wohlers T, Gornet T. History of additive manufacturing. Wohlers report. 2014;24(2014):118.

[5] Maidin S, Yi T, Hambali A, Akmal S, Hambali R, Abdullah Z. Investigation of optimum gating system design of fused deposition modelling pattern for sand casting. Journal of Mechanical Engineering and Sciences. 2017;11(3):2801-14.

[6] Šljivić M, Kraišnik M, Ilić J, Anić J. Development of Small Batches of Functional Parts Using Integration of 3D Printing and Vacuum Casting Technology. Acta Technica Corvininesis-Bulletin of Engineering. 2018;11(2).

[7] Singh J, Bagde P, Soni S, Verma JK, Kalyan K. Investigations on dimensional accuracy and surface finish of polyurethane replicas fabricated by silicon molding process for rapid casting applications. International Journal of Mechanical Engineering and Technology. 2017;8(7):1676-83.

[8] Singh J, Singh R, Singh H. Experimental investigations for dimensional accuracy and surface finish of polyurethane prototypes fabricated by indirect rapid tooling: a case study. Progress in Additive Manufacturing. 2017;2(1-2):85-97.

[9] Guo H, Zhou YT. The CAE Analysis for Thin-Walled Plastic Parts Vacuum Casting. Advanced Materials Research. 2014;889-890:52-7.

[10] Puerta APV, Sanchez DM, Batista M, Salguero J. Criteria selection for a comparative study of functional performance of Fused Deposition Modelling and Vacuum Casting processes. Journal of Manufacturing Processes. 2018; 35:721-7.

[11] Zamani J, Hemati M, Morsaluie R. An experimental comparison on dimensional accuracy of wax patterns of gas turbine blades produced by rapid tooling. Arabian Journal for Science and Engineering. 2014;39(10):7289-97.

[12] Iftikhar A, Khan M, Alam K, Imran Jaffery SH, Ali L, Ayaz Y, et al. Turbine blade manufacturing through rapid tooling (RT) process and its quality inspection. Materials and Manufacturing Processes. 2013;28(5):534-8.

[13] Budzik G, Markowski T, Sobolak M. Hybrid foundry patterns of bevel gears. Archives of Foundry Engineering. 2007;7(1):131-4.

[14] Sever-Adrian R, Frăţilă D-F. Simulation and Experimental Research on the Vacuum Casting of Non-Metallic Complex Parts Using Flexible Molds.

[15] Vosniakos G-C, Michael S, Vasileiou A. Digital Manufacturing Process Chain for One-Off Replacement Parts: A Precision Casting Case Study. Journal of Manufacturing and Materials Processing. 2017;1(2):17.

[16] Ahmad MN, Alkahari MR, Basir MFM, Maidin NA, Wahid MK, Ab Rahman MH. Optimization of vacuum casting process parameters using Taguchi method. Proceedings of Mechanical Engineering Research Day 2018; 2018.

[17] Chang DY, Deng CS. Process Parameter Experiments on Vacuum Casting Using a Silicone Rubber Mold for ABS Plastic Parts. Advanced Materials Research. 2011;201-203:1668-71.

[18] Aggenbacht FC. Development and Evaluation of a Vacuum Casting Process

2004.

[19] Tang Y, Tan WK, Fuh JYH, Loh HT, Wong YS, Thian SCH, et al. Micro-mould fabrication for a micro-gear via vacuum casting. Journal of Materials Processing Technology. 2007;192-193:334-9.

[20] Sabdin S, Hussein N, Sued M, Ayob M, Rahim M, Fadzil M. Effects of ColdArc welding parameters on the tensile strengths of high strength steel plate investigated using the Taguchi approach. Journal of Mechanical Engineering and Sciences. 2019;13(2):4846-56.

[21] Griffiths B. 5 - Limits, Fits and Geometrical Tolerancing. In: Griffiths B, editor. Engineering Drawing for Manufacture. London: Butterworth-Heinemann; 2003. p. 88-110.

[22] Bassoli E, Gatto A, Iuliano L, Grazia Violante M. 3D printing technique applied to rapid casting. Rapid Prototyping Journal. 2007;13(3):148-55.

[23] Minetola P, Iuliano L, Marchiandi G. Benchmarking of FDM machines through part quality using IT grades. Procedia CIRP. 2016; 41:1027-32.

[24] Ali MY, Banu A, Salehan M, Adesta EY, Hazza M, Shaffiq M. Dimensional accuracy in dry micro wire electrical discharge machining. Journal of Mechanical Engineering and Sciences. 2018;12(1):3321-9.